Electronic Supplementary Material (ESI) for Analytical Methods.

Supporting Information

A bifunctional fluorescent probe for sensing of Al^{3+} and H_2S

Ziao Zong, Jing Wang, Yidong Bin, Yanliu Wu, Guimei Huang*

School of Laboratory Medicine, Youjiang Medical University for Nationalities, Baise, 533000 Guangxi, China

standard-addition method (n =3).

Table S4 Determination of H_2S in water samples from different water sources by standard-addition method (n =3).

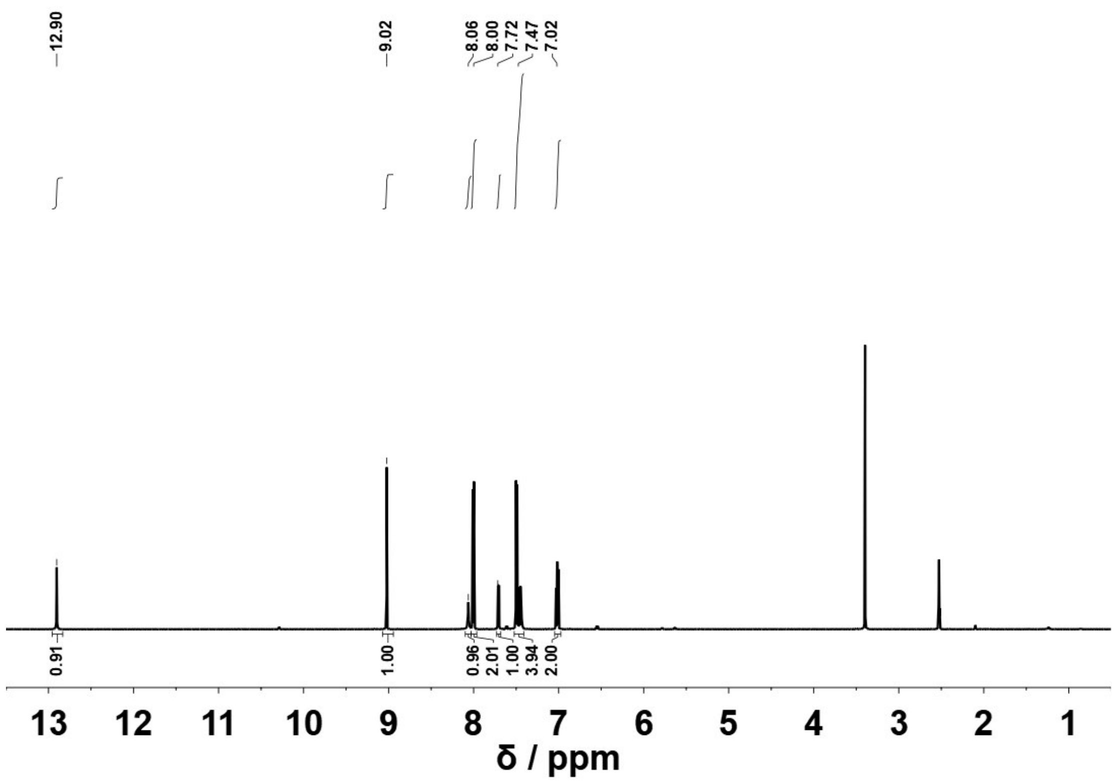

Fig. S1. ^{1}H NMR (DMSO-d_6, 600 MHz) spectrum of **L**.

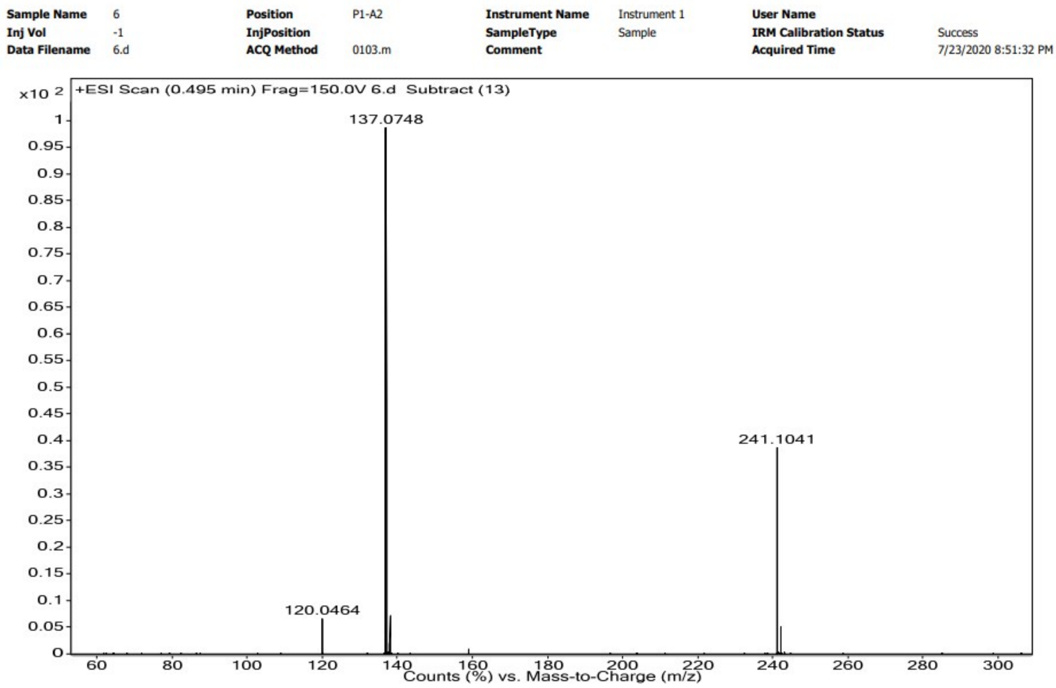

Fig. S2. The ESI-MS spectrum of compound **L.**

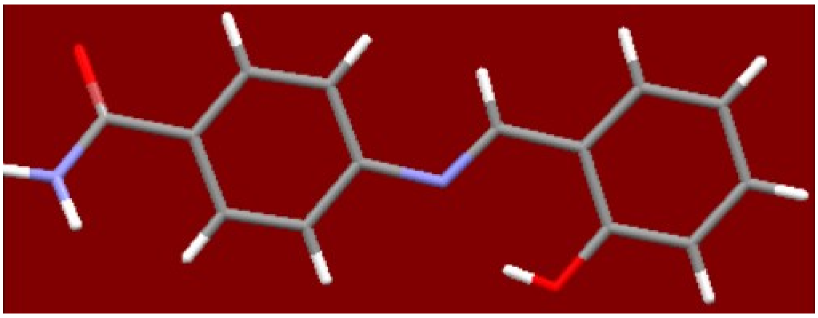

Fig. S3. The dihedral angle of **L.**

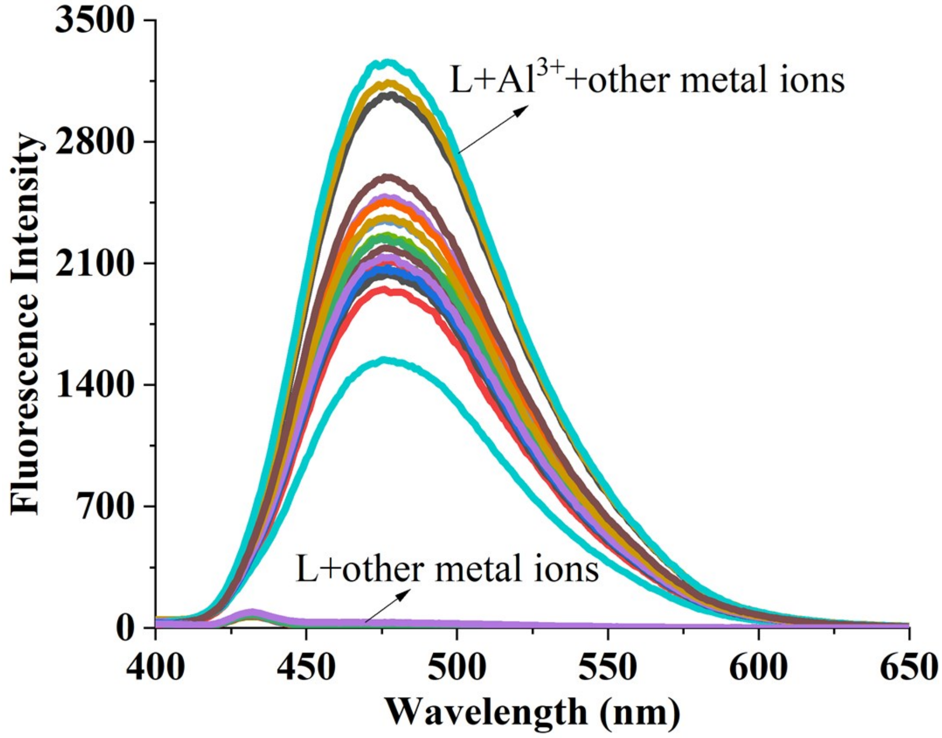

Fig. S4. Competition experiment of L toward Al^{3+} in the presence of 5 equiv. of other metal ions in MeOH/H_2O (9/1, v/v, pH=7.4), λex = 380 nm.

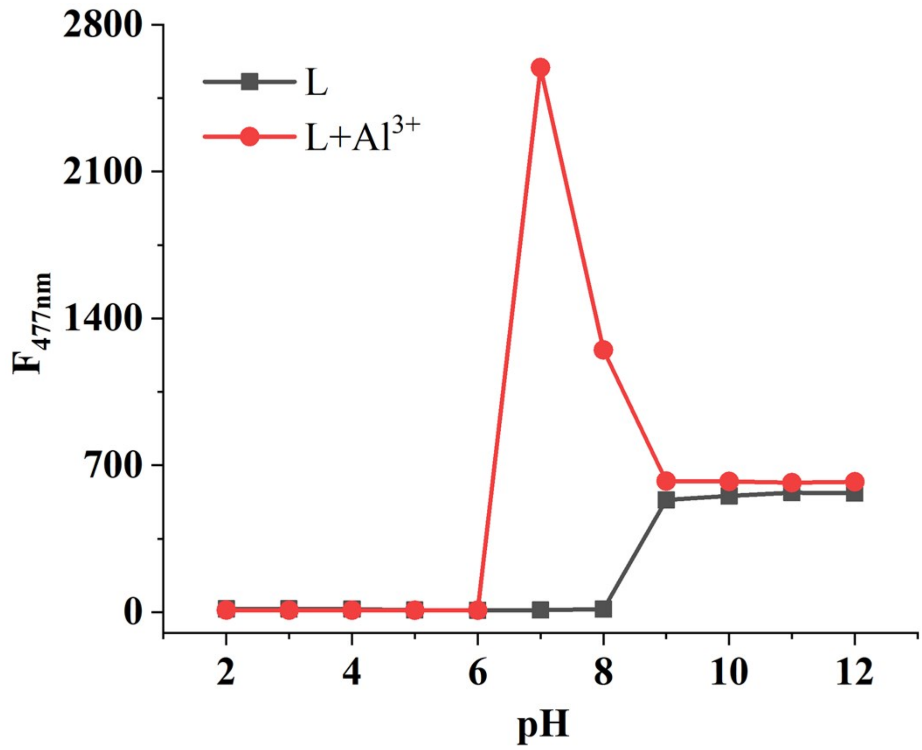

Fig. S5. Fluorescence intensity at 477 nm of **L** (10 μM) at various pH values in MeOH/H_2O (9/1, v/v) medium in the absence and presence of Al^{3+} (5 equiv).

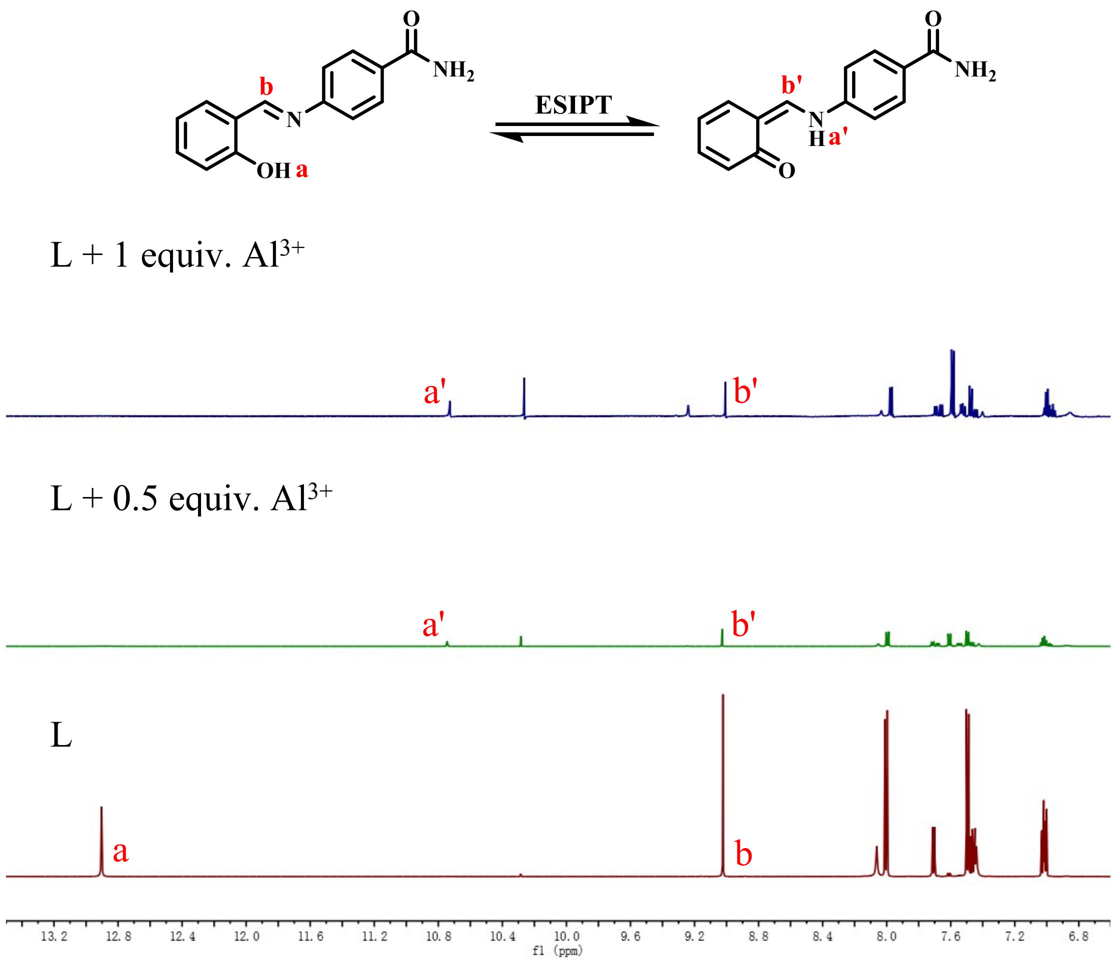

Fig. S6. ^{1}H NMR (DMSO-d_6, 600 MHz) spectra of **L** with Al^{3+}.

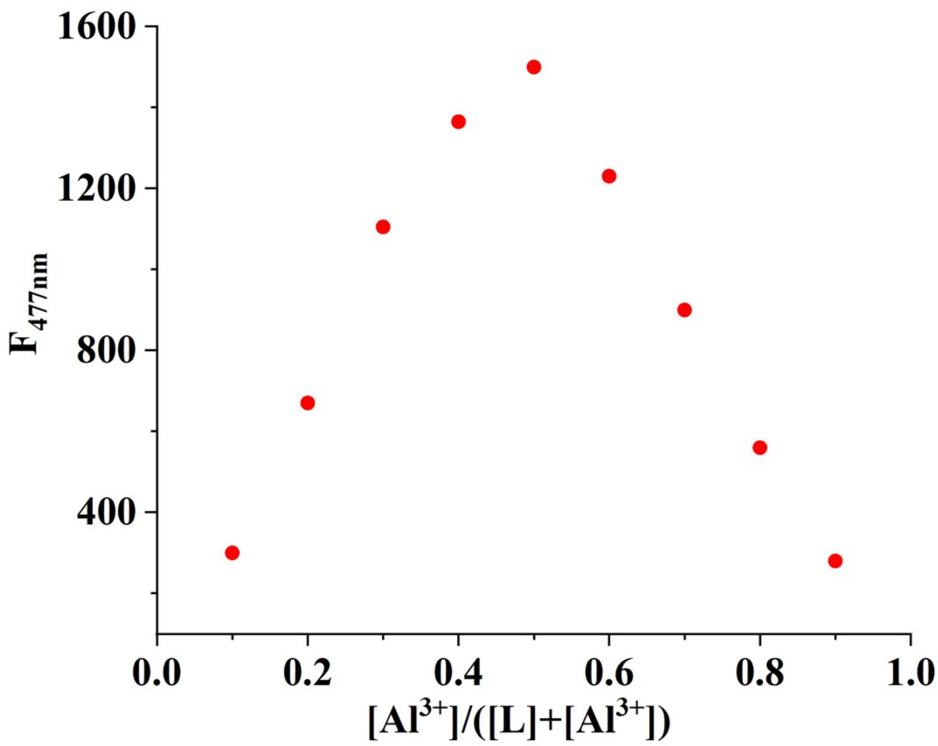

Fig. S7. Job's plot of **L**-Al^{3+} system in MeOH/H_2O (9/1, V/V, pH=7.4) medium.

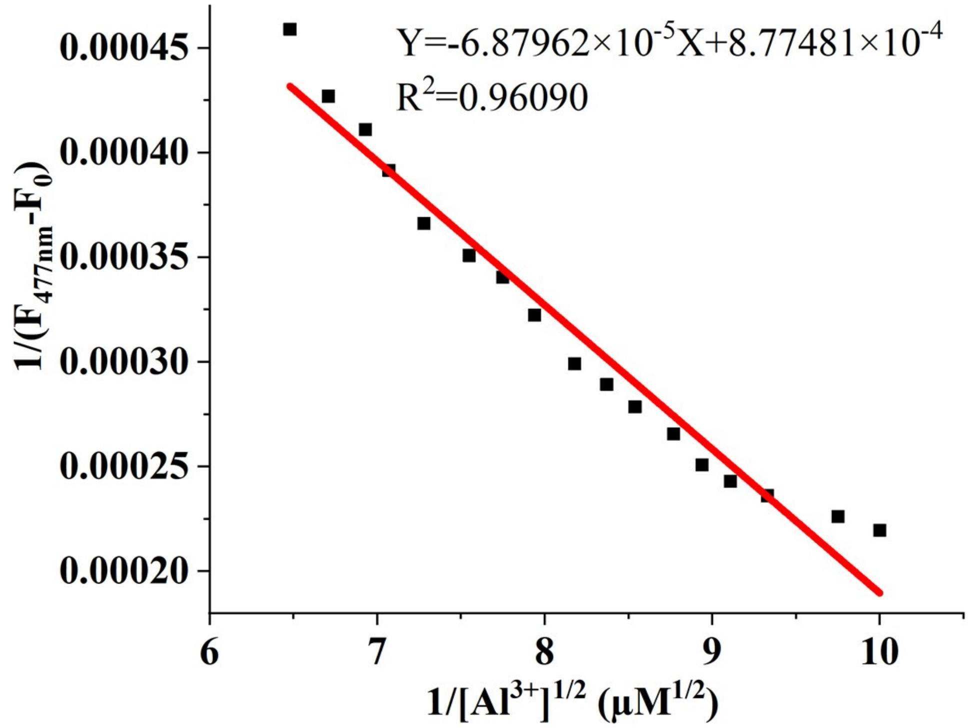

Fig. S8. Benesi-Hildebrand plot of **L**-Al^{3+} system in MeOH/H_2O (9/1, v/v, pH=7.4) medium.

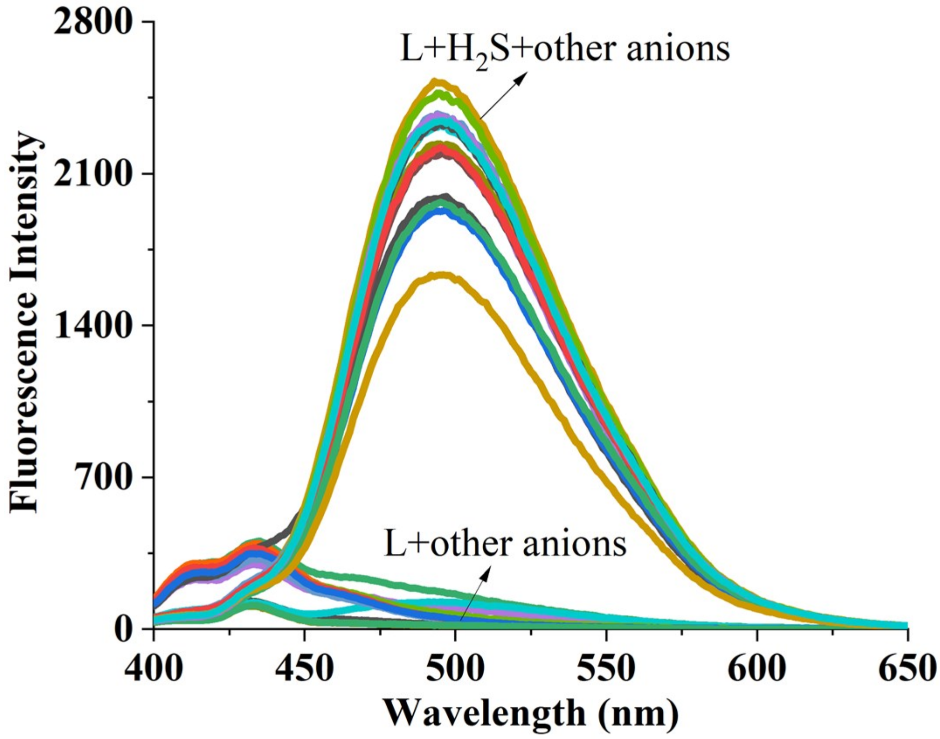

Fig. S9. Competition experiment of L toward H_2S in the presence of 5 equiv. of other anions in EtOH/H_2O (7/3, v/v, pH=7.4).

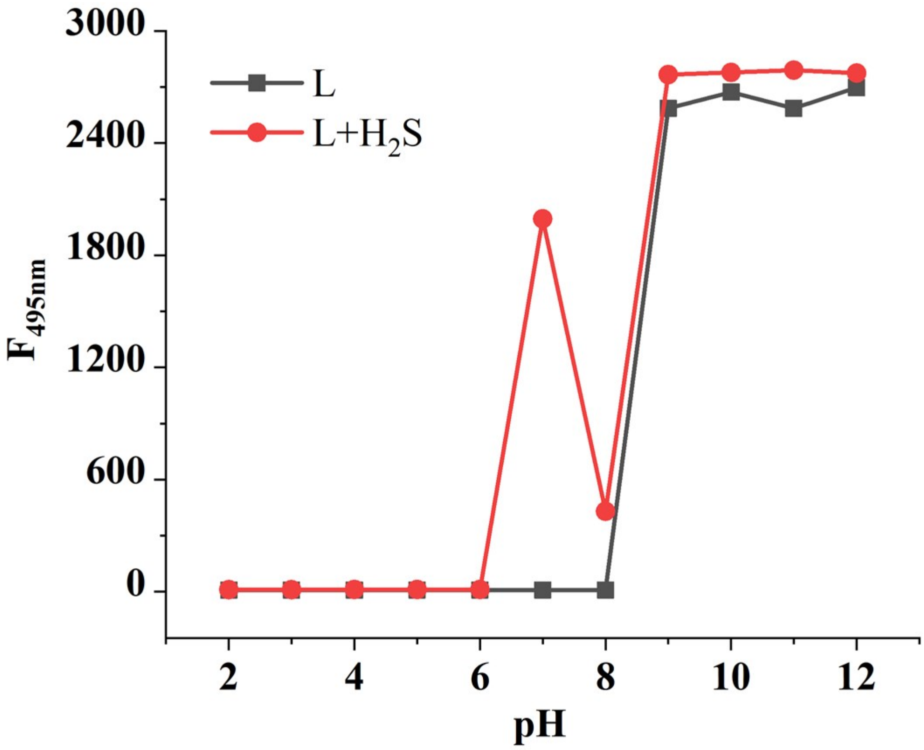

Fig. S10. Fluorescence intensity at 495 nm of **L** (10 μM) at various pH values in EtOH/H_2O (7/3, v/v) medium in the absence and presence of H_2S (5 equiv).

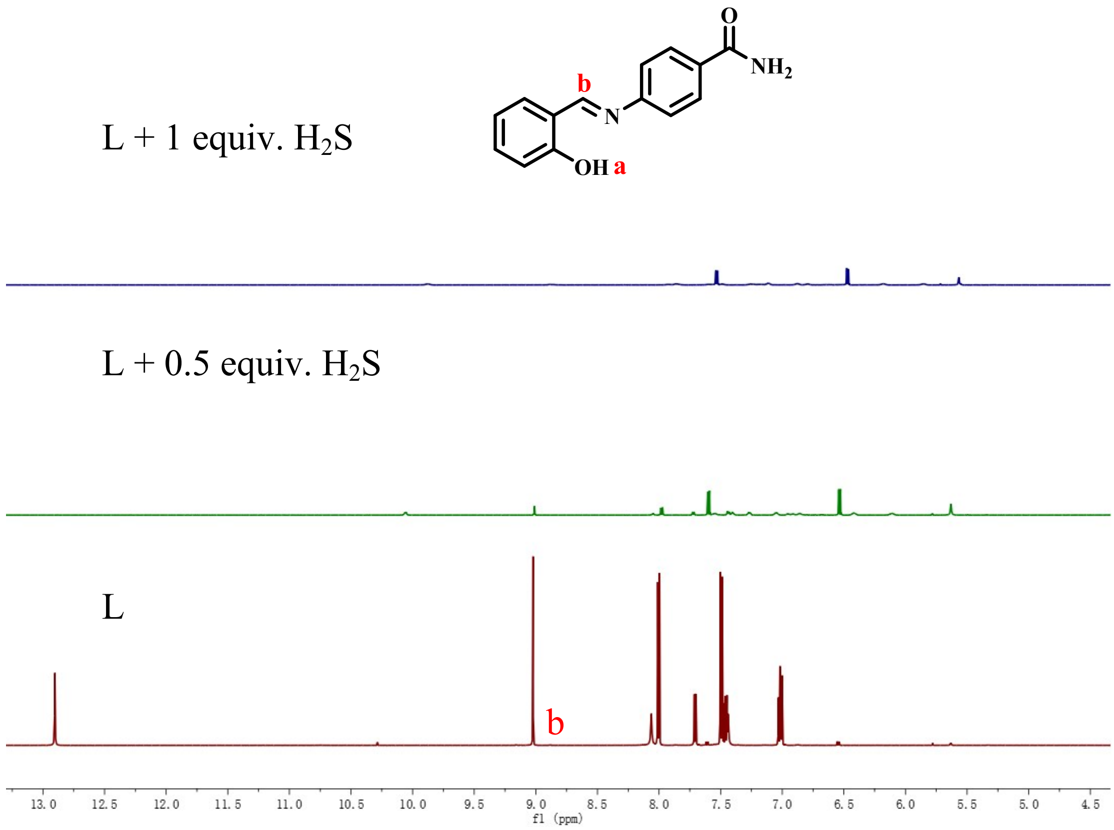

Fig. S11. [1]H NMR (DMSO-d_6, 600 MHz) spectra of **L** with H_2S.

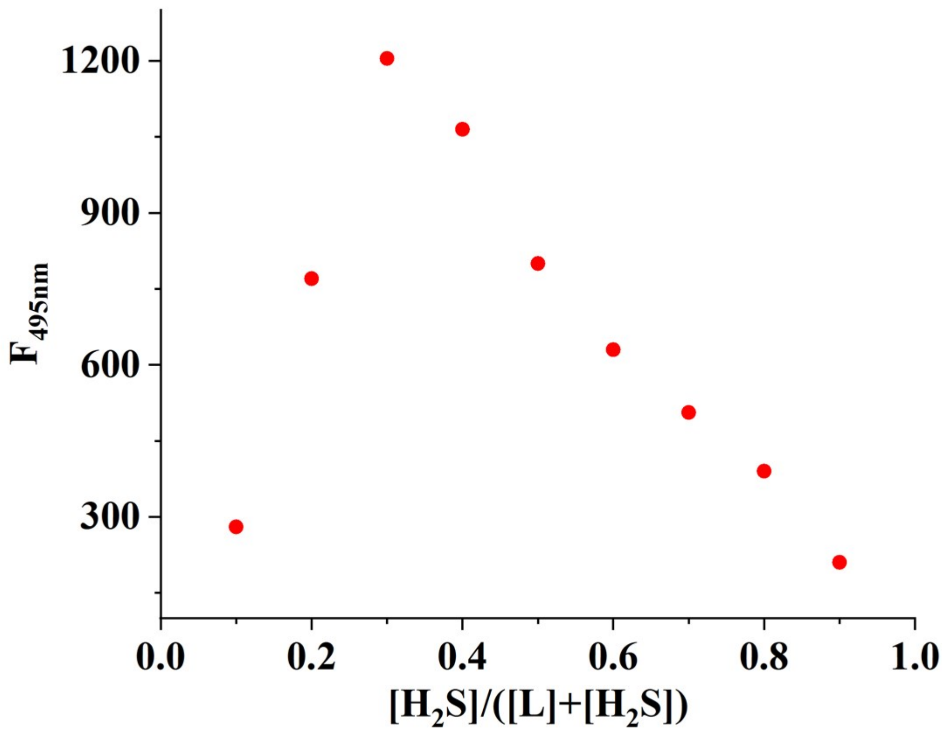

Fig. S12. Job's plot of **L**-H_2S system in EtOH/H_2O (7/3, V/V, pH=7.4) medium.

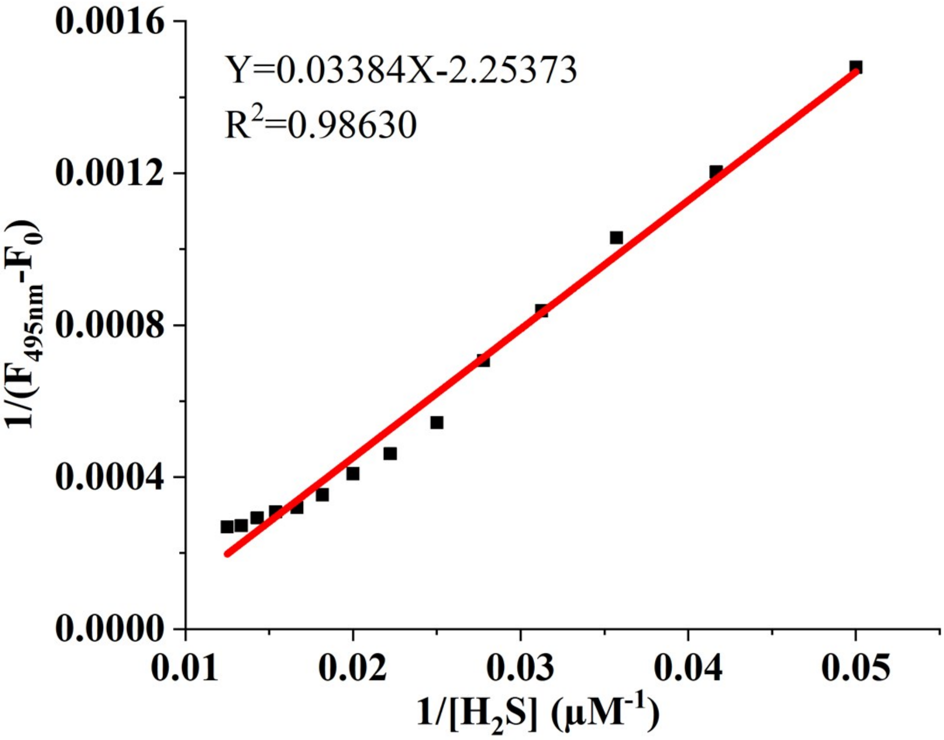

Fig. S13. Benesi-Hildebrand plot of **L**-H_2S system in EtOH/H_2O (7/3, v/v, pH=7.4) medium.

Table S1 Summary of crystal data and structure refinement parameters for **L**

Crystal data	
Empirical formula	$C_{14}H_{12}N_2O_2$
Formula weight	240.26
Crystal system, space group	Monoclinic, $P2_1/n$
Temperature (K)	100
a, b, c (Å)	5.0646 (4), 5.1677 (5), 43.549 (4)
β (°)	92.595 (4)
V (Å^3)	1138.61 (18)
Z	4
Radiation type	Mo $K\alpha$
μ (mm^{-1})	0.096
Crystal size (mm)	0.19 × 0.15 × 0.12
$\Delta\rho_{max}$, $\Delta\rho_{min}$ (e Å^{-3})	0.29, -0.27

Table S2 Selected bond lengths (Å) and angles (°) for **L**.

Bond lengths (Å)		bond angles (°)	
O1—C14	1.2462 (18)	C7—N1—C8	121.93 (14)
O2—C1	1.346 (2)	O2—C1—C2	119.40 (15)
N1—C7	1.278 (2)	C2—C1—C6	119.51 (15)
N2—C14	1.3338 (19)	C5—C6—C1	118.23 (15)
C1—C2	1.393 (2)	C5—C6—C7	120.40 (15)
C1—C6	1.397 (2)	N1—C7—C6	121.90 (15)
C5—C6	1.397 (2)	C10—C9—C8	120.84 (15)
C8—C9	1.388 (2)	C9—C10—C11	120.24 (15)
C10—C11	1.392 (2)	O1—C14—N2	122.34 (12)
C11—C12	1.390 (2)	N2—C14—C11	117.30 (13)

Table S3 Determination of Al^{3+} in water samples from different water sources by standard-addition method (n =3).

Water samples studied	Amount of standard Al^{3+} added (μM)	Total Al^{3+} found (n=3) (μM)	Recovery of Al^{3+} (n=3) added (%)	RSD (%)	Relative error （%）
Tap water	3.0	3.02	100.67	1.20	1.75
	3.5	3.48	99.43	0.65	-1.18
	4.0	4.03	100.75	2.57	0.86
	4.5	4.48	99.56	1.36	-1.62
	5.0	4.97	99.40	1.56	-2.16
	5.5	5.56	101.09	0.78	0.69
Lake water	3.0	3.01	100.33	1.72	1.06
	3.5	3.53	100.86	2.00	3.18
	4.0	3.95	98.75	1.56	-0.59
	4.5	4.54	100.89	1.25	1.76
	5.0	4.89	97.80	0.26	-2.35
	5.5	5.60	101.82	0.38	2.16

Table S4 Determination of H_2S in water samples from different water sources by standard-addition method (n =3).

Water samples studied	Amount of standard H_2S added (μM)	Total H_2S found (n=3) (μM)	Recovery of H_2S (n=3) added (%)	RSD (%)	Relative error （%）
Tap water	6.0	5.96	103.80	2.20	2.75
	6.5	6.48	95.70	0.50	-2.18
	7.0	6.95	102.87	3.57	0.63
	7.5	7.42	98.90	1.50	-1.82
	8.0	7.91	97.36	2.56	-3.12
	8.5	8.53	97.17	0.30	-0.78
Lake water	6.0	6.04	101.80	1.60	2.07
	6.5	6.51	103.30	3.00	3.28
	7.0	6.92	95.67	1.16	-2.59
	7.5	7.52	104.35	3.75	1.62
	8.0	8.05	102.60	0.16	2.68
	8.5	8.46	95.60	0.29	-2.66